High temperature treatment of ordered mesoporous carbons prepared by using various carbon precursors and ordered mesoporous silica templates†

Kamil P. Gierszal,[a] Mietek Jaroniec,*[a] Tae-Wan Kim,[b] Jeongnam Kim[b] and Ryong Ryoo*[b]

Received (in Montpellier, France) 30th October 2007, Accepted 19th December 2007
First published as an Advance Article on the web 23rd January 2008
DOI: 10.1039/b716735k

The effect of high temperature treatment of ordered mesoporous carbons (OMCs) under neutral atmosphere is studied for OMCs prepared by using different carbon precursors (furfuryl alcohol, sucrose, acenaphthene and mesophase pitch) and different ordered mesoporous silica (OMS) templates (MCM-48 and KIT-6). The OMS-templated carbons were thermally treated at various temperatures ranging from 900 °C to 2400 °C to study changes in their porosity and framework crystallinity. The KIT-6 silica was synthesized at different conditions to control the size of primary mesopores and interconnecting complementary pores. The use of MCM-48 silica as template afforded the carbon replicas, CMK-1, which underwent a structure transition from $Ia\bar{3}d$ to $I4_1/a$. The use of the KIT-6 silica template, depending on the size of complementary pores, afforded a faithful inverse replica, CMK-8, as well as the CMK-1-type structure that underwent the aforementioned symmetry transition. The XRD patterns for the carbons studied showed that their thermal treatment led to a gradual deterioration of the carbon structure, which was associated with structure shrinking and pore walls fracturing. Particularly significant changes in the structural properties of the carbons studied occurred for those heated (graphitized) at 2400 °C, which manifested itself in a partial or complete loss of the pore volume. It was found that the CMK-1-type graphitized carbons exhibited better thermal stability, which is reflected by the presence of residual mesopores and/or nanostructure ordering. The degree of graphitization for the carbons heated at 2400 °C depended insignificantly on the type of carbon precursor; however, the precursor effect became more pronounced with decreasing temperature of the thermal treatment.

Introduction

Graphitized nanoporous carbons have attracted a lot of attention because they combine characteristic features of nanoporous carbons such as chemical inertness, high surface area and high pore volume with good electrical conductivity and high surface homogeneity created by graphitization process. These features make porous graphitized carbons (PGCs) attractive materials for advanced adsorption, catalysis and electrochemical applications. In general, porous carbons with graphitic framework can be synthesized by a two-step process involving the formation of a nanoporous carbon and its subsequent high temperature treatment under inert atmosphere, which is known as graphitization.

Recently, there has been a great interest in ordered nanoporous carbons, which are usually synthesized by hard templating method.[1–5] This synthesis strategy includes: (i) partial or complete filling of porous silica template with a carbon precursor by infiltration, chemical vapor deposition (CVD) or otherwise, (ii) carbonization of the carbon precursor inside porous silica at temperature usually below 1000 °C, and (iii) removal (dissolution) of silica from the carbon–silica composite. Depending on the type of carbon precursor, catalyst and temperature used, the resulting porous carbon can be partially graphitized, which is reflected by the presence of short-range crystalline (graphite-like) domains, or can be totally amorphous. The formation of graphite-like domains can be facilitated by using aromatic and polyaromatic compounds such as divinylbenzene, pyrole, petroleum pitch and mesophase pitch as carbon precursors and heating the material at temperature of ~900 °C or higher.[6–14] Porous carbons with graphite-like domains can be obtained from nonaromatic carbon precursors but in this case high temperatures (1600 °C or higher) are required.[15] Also, it was shown that the introduction of nitrogen-containing carbon precursors (*e.g.*, acetonitrile) into pores of the silica template by chemical vapor deposition (CVD) followed by carbonization at 950 °C afforded partially graphitized porous carbons.[16] However, to achieve a high degree

[a] *Department of Chemistry, Kent State University, Kent, Ohio 44242, USA. E-mail: jaroniec@kent.edu; Tel: 1-330-672 3790*
[b] *Center for Functional Nanomaterials and Department of Chemistry (School of Molecular Science BK21), KAIST, Daejeon 305-701, Republic of Korea. E-mail: rryoo@kaist.ac.kr*

† Electronic supplementary information (ESI) available: Fig. ESI-1 showing nitrogen low pressure adsorption isotherms in a semi-logarithmic scale for four series of carbons studied; Fig. ESI-2 and ESI-3 showing the TG and DTG curves and Fig. ESI-4 displaying Raman spectra for two series of carbons. See DOI: 10.1039/b716735k

of graphitization in a reasonable time it is necessary to subject porous carbons to the high temperature treatment (2400 °C or higher) in an atmosphere of inert gas.[17,18] In practice, PGCs can be fabricated in argon atmosphere at a temperature of about 2500 °C or higher during 0.5–1 h. The graphitization process under such conditions often leads to the collapse of porous structure or to a substantial reduction of the specific surface area and pore volume, which is due to the disappearance of numerous micropores and to the overall shrinkage of the porous structure.

The first report on the preparation of PGCs was published in 1986 by Knox *et al.*[19] The resulting PGC material was synthesized by using phenol–formaldehyde as carbon precursor and porous silica beads as hard template. In 2001 Li *et al.* applied mesophase pitch as carbon precursor and monodisperse silica colloids as hard template.[12,19,20] The colloid-templated carbon was graphitized at 2400 °C, which reduced by about 30–50% all adsorption parameters due to the structure shrinkage.[21] Despite that, the resulting PGC still possessed a relatively large total pore volume, high specific surface area and large pore size equal to 0.72 $cm^3\ g^{-1}$, 240 $m^2\ g^{-1}$ and 16 nm, respectively. Three years later, Fuertes *et al.* reported nanoporous carbons obtained by carbonization and subsequent graphitization at 2300 °C of poly(vinyl chloride) introduced to the ordered channels of SBA-15 and disordered pores of MSU-1 silica templates.[22] It appeared that the SBA-15-templated carbon possessed only partial ordering of mesopores and a high degree of graphitization, as assessed by small- and wide-angle X-ray diffraction (XRD). This carbon had a quite high surface area of 260 $m^2\ g^{-1}$ and a moderate pore volume of 0.32 $cm^3\ g^{-1}$. The first fully graphitized well-ordered nanoporous carbon was synthesized from mesophase pitch incorporated into pores of colloidal silica crystals formed from ~69 nm colloids.[23] Graphitization of this mesoporous carbon at temperature of 2500 °C caused a noticeable shrinkage of the structure but its ordered porosity was preserved as shown by nitrogen adsorption and transmission electron microscopy (TEM). Raman and wide angle X-ray diffraction spectra as well as low pressure nitrogen adsorption and high resolution TEM confirmed a high degree of graphitization of this colloid-templated carbon. More recently Kruk *et al.* reported partially graphitized carbons at 2200 °C templated by using ordered SBA-15 and FDU-1 silicas as well as disordered silica gel Si-150.[24] Acrylonitrile, used as carbon precursor, was introduced into the pores of the aforementioned silicas and polymerized *via* surface-initiated atom transfer radical polymerization (ATRP). The resulting ordered mesoporous carbons (OMCs) were subjected to high temperature treatment, which caused a significant shrinkage leading to a decrease in the pore volume, broadening of pore size distribution (PSD) and a loss of nanoscale ordering. In the case of the disordered carbon, temperature treatment at 2200 °C markedly decreased the amount of micropores in the framework but did not change its total pore volume. Partial graphitization of these polyacrylonitrile-based carbons was confirmed by XRD, Raman spectroscopy, and TEM.

An attractive alternative to the high temperature graphitization (above 2000 °C) is graphitization performed at lower temperatures (800–900 °C) but in the presence of catalysts.[25–30] Typically, the transition metal nanoparticles such as cobalt, nickel or iron embedded in the carbon framework or deposited on its surface are used as catalysts to facilitate graphitization at low temperatures, which is usually used for the carbonization of various carbon precursors. This catalyzed graphitization is undoubtedly advantageous because it eliminates harsh graphitization conditions and shortens the time of carbon preparation but, on the other hand, an additional preparation step might be necessary for the removal of catalyst from the pores. Moreover, a drawback of the catalyst removal can be the creation of undesired secondary porosity in the carbon framework.

In this work, ordered mesoporous silicas (OMSs) such as MCM-48[31] and KIT-6[32,33] are used as hard templates for the synthesis of carbons *via* templating method. Both types of OMSs feature the same 3D cubic structure ($Ia\bar{3}d$ symmetry) consisting of an interpenetrating bicontinuous network of channels. The main difference between these OMS structures are larger pores in the KIT-6 silica formed by using a non-ionic poly(ethylene oxide)–poly(propylene oxide)–poly(ethylene oxide) triblock copolymer template with addition of *n*-butanol. However, from the viewpoint of the OMC synthesis, another and more important difference between these silica templates is the presence of irregular small pores (mostly micropores that interconnect the aforementioned bicontinuous channels) in the KIT-6 mesopore walls, which are analogous to the complementary pores in SBA-15 (2D hexagonally ordered OMS).[34,35] Because the cationic surfactant-templated MCM-48 silica does not normally possess those complementary pores, it is difficult to obtain its faithful inverse replica. Any attempt of using MCM-48 as hard template for the replication-type synthesis causes a symmetry change from $Ia\bar{3}d$ to $I4_1/a$ (or lower group) in the replica obtained by silica removal; this change is associated with the pore enlargement caused by displacement of the formerly separated replicas of each enantiomeric porous system.[36] In the case of KIT-6, an adjustment of suitable synthesis conditions can be used, such as temperature, SiO_2/polymer ratio and time of hydrothermal treatment (see details elsewhere),[33,37] in order to control not only the size of the primary mesopores but also the size and volume of interconnecting complementary pores. Since the latter can be tailored in the range from zero (*i.e.*, low temperature hydrothermal treatment, <70 °C) to several nanometers, it is feasible to synthesize ordered mesoporous carbon (OMC), known as CMK-8, being a faithful inverse replica of KIT-6 ($Ia\bar{3}d$),[13,37] as well as OMCs with large mesopores formed by the aforementioned structure transformation, which permits mesopores of about 10 nm to be obtained.

This study is focused on the adsorption and structural properties of OMS-templated OMCs subjected to thermal treatment at temperatures of 900, 1200, 1600, 2000 and 2400 °C. The OMC studied were synthesized from polyaromatic acenaphthene and mesophase pitch as well as non-aromatic furfuryl alcohol and sucrose. The high temperature treatment of these OMCs allowed us to monitor the structural transformations during carbonization graphitization processes depending on the type of the carbon precursors and OMS templates used and to identify the best carbon precursors,

OMS templates and experimental conditions for the synthesis of PGCs.

Experimental

Preparation of MCM-48 and KIT-6 silica templates

Mesoporous silicas, MCM-48, were prepared using a mixture of *n*-alkyltrimethylammonium bromide (C_nTMABr)–co-surfactant as a soft template and a sodium silicate solution (9 wt% aqueous solution, Na/Si = 0.5) as a silica source. The detailed synthesis was described elsewhere.[38,39] In brief, the surfactant solution and the silica source were rapidly mixed under vigorous shaking for 30 min at room temperature. Subsequently, the resulting synthesis gel was heated at 100 °C for 43 h and cooled down to room temperature. Its pH was adjusted to 10 by adding acetic acid, and finally the gel was heated at 100 °C for 48 h before filtration of the product. The as-synthesized samples were washed with ethanol–HCl and calcined. The resultant MCM-48 silica products are denoted by MCM48-C*n* (where C*n* refers to the alkyl chain length in C_nTMABr).

The starting molar ratios were 5.0 SiO_2 : 1.25 Na_2O : 0.75 C_{12}TMABr : 0.25 LE-3 : 300 H_2O and 5.0 SiO_2 : 1.25 Na_2O : 0.92 C_{20}TMABr : 0.08 Triton X-100 : 300 H_2O for C_{12}MCM-48 and C_{20}MCM-48, respectively (where LE-3 and Triton X-100 denote $C_{12}H_{25}O(C_2H_4O)_3H$ and $CH_3C(CH_3)_2CH_2$-$C(CH_3)_2$ $C_6H_4O(C_2H_4O)_{10}H$, respectively). The C_{12}TMABr and LE-3 were obtained from Hannong Chemical and Triton X-100 from Daejung Chemical, and C_{20}TMABr was synthesized at KAIST.[40]

Large-pore cubic $Ia\bar{3}d$ mesoporous silicas, KIT-6, were synthesized according to the procedure described elsewhere.[32,33] Briefly, Pluronic P123 ($EO_{20}PO_{70}EO_{20}$, Aldrich) and *n*-butanol (Aldrich) were mixed in aqueous HCl solution. After complete dissolution of the polymer, tetraethyl orthosilicate (TEOS, Acros) was added into the mixture at 35 °C under magnetic stirring, which was continued for 1 d at the same temperature. Subsequently, the mixture was heated for 1 d in an oven for hydrothermal treatment. After the hydrothermal treatment, the solid product was recovered by filtration and dried without washing. The as-synthesized KIT-6 materials were washed with an ethanol–HCl mixture and finally calcined. The molar compositions of the starting reaction mixture were 0.017 P123 : *x* TEOS : *y* BuOH : 1.83 HCl : 195 H_2O, where [*x*, *y*] = [1.2, 1.31] and [2.0, 2.10]. The hydrothermal temperatures were 35 and 130 °C depending on the samples. The resultant products are denoted as KIT6-*x*-T, where *x* refers to TEOS molar ratio and T denotes temperature of the hydrothermal treatment. For example, KIT6-1.2-35 was synthesized by using the composition of 0.017 P123 : 1.2 TEOS : 1.31 BuOH : 1.83 HCl : 195 H_2O at 35 °C. To prepare KIT-6 in an aluminosilicate form (denoted by Al-KIT6-*x*-T), the products were impregnated with Al using an aqueous solution of $AlCl_3$ (Si/Al = 20) before calcination.[41]

Synthesis of mesoporous carbons by using MCM-48 template

Mesoporous carbon, CMK-1, obtained by filling the channels of MCM-48 with furfuryl alcohol was prepared as reported elsewhere,[36,42] except carbonization, which was performed under 1 atm instead of vacuum conditions, and *p*-toluene sulfonic acid (TS) used as an acid catalyst. According to this recipe, infiltration of furfuryl alcohol was repeated twice prior to carbonization. Briefly, this recipe was as follows: 1 g of MCM48-C12 was infiltrated with 0.87 mL of furfuryl alcohol containing 1.92 mg of TS catalyst at room temperature. The resultant sample was heated for 1 h at 35 °C, 1 h at 100 °C, and then 2 h at 350 °C. After cooling down the sample to room temperature, 0.61 mL of furfuryl alcohol containing 1.35 mg of TS catalyst was added; the resulting mixture was heated at 100 °C, and later at 350 °C. Carbonization was accomplished by further heating to 900 °C. The heat treatments were performed under self-generated, non-combustive atmosphere, using fused quartz tubing equipped with a porous plug. After HF washing, the collected carbon products obtained by using MCM48-C12 and MCM48-C20 templates were denoted as CMK1-C12-FA and CMK1-C20-FA, respectively, where CMK-1 refers to the carbon structure generated during MCM-48-templating synthesis (this kind of structure is formed after silica removal from the MCM-48–carbon composite, which is accompanied by symmetry transition from $Ia\bar{3}d$ to $I4_1/a$. C12 and C20 refer to the alkyl chain lengths in the C_nTMABr template used to obtain MCM-48 and FA denotes furfuryl alcohol used as carbon precusor.

Synthesis of mesoporous carbons by using KIT-6 template

Four types of carbons were synthesized by using KIT-6 and different carbon precursors. First, the KIT-6-templated carbon was prepared from furfuryl alcohol carbon precursor according the same recipe as that used to obtain CMK-1 samples (see previous section) except for the difference in the amount of furfuryl alcohol. Briefly, the TS catalyst (4.3 mg per gram of furfuryl alcohol) was mixed with furfuryl alcohol (0.46 and 0.31 mL per gram of KIT6-1.2-35 template in the 1st and 2nd impregnation, respectively) and the resulting mixture was impregnated into the KIT-6 template at room temperature. The remainder of the recipe is the same as that used to obtain CMK-1 carbons. The carbon product is denoted as CMK1-LP-FA. Note that the same designation, CMK-1, was used for both kinds of carbons templated by employing MCM-48 and KIT-6 silicas because they feature a similar symmetry transition from $Ia\bar{3}d$ to $I4_1/a$. LP stands for large pore and indicates templating by means of the KIT-6 silica, while FA denotes furfuryl alcohol. CMK1-LP is also used for designating other carbon samples described below.

The second mesoporous carbon was prepared by using the AR mesophase pitch according to the previously reported recipe;[13] namely, 0.92 g of the AR mesophase pitch (softening point 285 °C, donated by Mitsubishi Gas Chemical Co., Japan) and 1 g of pure KIT-6-1.2-35 were mixed together in polypropylene bottle with 10 mL of ethanol. After agitation of this mixture for 30 min, ethanol was evaporated at 100 °C in an oven. The dry mixture was moved to a quartz reactor equipped with porous plug and heated in a furnace at 300 °C. After maintaining the aforementioned infiltration temperature for 4 h, the mixture was heated to 900 °C under nitrogen. The product was collected after the quartz reactor had cooled

down to room temperature. The resultant product was recovered by removal of the silica template with HF acid. The samples are denoted as CMK1-LP-MP, where MP denotes mesophase pitch. In an analogous way, the CMK8-MP carbon was prepared with the use of the KIT-6-1.2-130C silica template.

The third carbon was prepared by using sucrose as carbon precursor according to a similar procedure as that used for the original synthesis of CMK-1,[35,36,42] except that the carbonization was carried out under a pressure of 1 atm instead of under vacuum. The amounts of sucrose and sulfuric acid (H_2SO_4) were also adjusted in relation to the pore volume. The pore volume of KIT6-1.2-35 silica is 0.72 $cm^3\ g^{-1}$. This sample was first infiltrated with a mixture consisting of 1.25 g sucrose, 0.077 mL H_2SO_4 and 1.3 g H_2O per gram of SiO_2. After heating at 160 °C, the resultant mixture was again infiltrated with 0.797 g of sucrose, 0.049 mL of H_2SO_4 and 1.1 g of H_2O. Carbonization was accomplished by heating at 900 °C under nitrogen. The carbon product was recovered after dissolution of the silica template with HF acid. This carbon is designated CMK1-LP-SU, where SU denotes sucrose.

The fourth carbon was obtained by using acenaphthene according to the previously reported recipe[13,14] except for the difference in the amount of carbon precursor, which was adjusted in relation to the pore volume of the silica template. The synthesis recipe was as follows: a mixture of 1.39 g of acenaphthene and 1 g of AlKIT6-1.2-130 was placed in an autoclave and heated at 750 °C in a muffle furnace. After being cooled down to room temperature, the product was moved into a fused quartz reactor, which was equipped with fritted disks. Carbonization was performed by heating the reactor at 900 °C in vacuum conditions. The carbon sample was filtered and subjected to the silica template removal with HF acid. This carbon is denoted as CMK8-AN, where AN denotes acenaphthene.

One more CMK1-LP sample was synthesized with furfuryl alcohol, similarly to CMK1-LP-FA. The difference from CMK1-LP-FA was that KIT6-2-35 was used as the silica template instead of KIT6-1.2-35, and the amount of FA was adjusted according to the total pore volume of the silica template (See Table 1 for pore volume). This sample is denoted as CMK1-LP*-FA.

High temperature heat treatment

All carbon samples were subjected to thermal treatment, which was done in a high temperature furnace (Ace Vacuum Co., Korea) under high purity Ar. The heat treatment was carried out at different temperatures: 1200, 1600, 2000, and 2400 °C for 1 h. Each temperature was achieved by using 5 °C per min heating rate. The resulting samples are denoted as CMK1-C12-FA-T, CMK1-C20-FA-T and CMK1-LP-P-T, where P refers to the carbon precursor used (= FA, MP, SU, AN) and T is the heat treatment temperature.

Table 1 The total pore volume (V_{tot}), BET specific surface area (S_{BET}), external surface area (S_{ext}) and pore size (w_{KJS}) for the MCM-48 and KIT-6 silicas used as hard templates for the synthesis of the carbons studied

Sample	V_{tot}/$cm^3\ g^{-1}$	S_{BET}/$m^2\ g^{-1}$	S_{ext}/$m^2\ g^{-1}$	w_{KJS}/nm
MCM48-C12	1.15	1120	170	3.49
MCM48-C20	1.27	1000	160	4.49
KIT6-1.2-130	1.27	590	30	11.65
KIT6-1.2-35	0.50	490	<10	5.95
KIT6-2-35	0.43	610	<10	4.71

Measurements and calculations

Synchrotron powder X-ray diffraction (XRD) patterns at small angle range were collected using BL8C2 at Pohang Light Source in the reflection mode (λ = 0.15444 nm). The XRD patterns at wide angle range were recorded on a Rigaku Multiplex instrument using Cu Kα radiation (λ = 0.15406 nm), operated at 50 kV and 30 mA (1.5 kW) in step scan mode. Transmission electron microscopy (TEM) images were taken from thin edges of particles supported on a porous carbon grid using JEOL JEM-2100F equipment operated at 200 kV.

Nitrogen adsorption isotherms were measured at −196 °C on a Micromeritics ASAP 2010 volumetric adsorption analyzer. Before adsorption measurements all samples were outgassed at 200 °C in the port of the adsorption analyzer. The BET specific surface area was calculated from nitrogen adsorption data in the relative pressure range from 0.04 to ~0.25 for silicas and from ~0.01 to ~0.15 for carbons. The total pore volume was estimated from the amount of nitrogen adsorbed at a relative pressure of about 0.99. The external surface area was estimated from nitrogen adsorption data using the α_s-plot method. The pore size distributions (PSDs) were calculated from adsorption branch data of nitrogen adsorption isotherms according to the KJS (Kruk, Jaroniec, Sayari) method developed for cylindrical pore geometry and calibrated by using a series of MCM-41 silicas.[43] The pore width was obtained at the maximum of PSD curve.

Thermogravimetric analysis was carried out in flowing air using a TA Instruments Inc. (New Castle, DE, USA) model TGA 2950 high-resolution thermogravimetric analyzer. The weight change (TG) curves were recorded over a temperature range from room temperature to 1000 °C. The instrument was equipped with an open platinum pan and an automatically programmed temperature controller. The high-resolution mode was used to record the TG data. The heating rate was adjusted automatically during measurements to achieve the best resolution; its maximum was 5 °C min^{-1}.

Results and discussion

Adsorption properties of silica templates

Fig. 1 shows the nitrogen adsorption isotherms for the OMS templates used for the synthesis of OMCs. Adsorption analysis (Table 1) indicates that the smallest pores and the highest specific surface area, 3.5 nm and 1120 $m^2\ g^{-1}$, respectively, were obtained for the MCM48-C12 silica synthesized by using the surfactant with the shortest chain. MCM48-C20 had a surface area of 1000 $m^2\ g^{-1}$ and somewhat larger pores (4.5 nm). Both samples are characterized by very narrow PSDs, indicating high uniformity of mesopores. In addition, both OMSs exhibited some textural (disordered and irregular) pores, whose volume was about 0.2 $cm^3\ g^{-1}$. The presence of the textural pores in these OMSs caused a decrease in the pore volume of their carbon replicas (expressed as the absolute

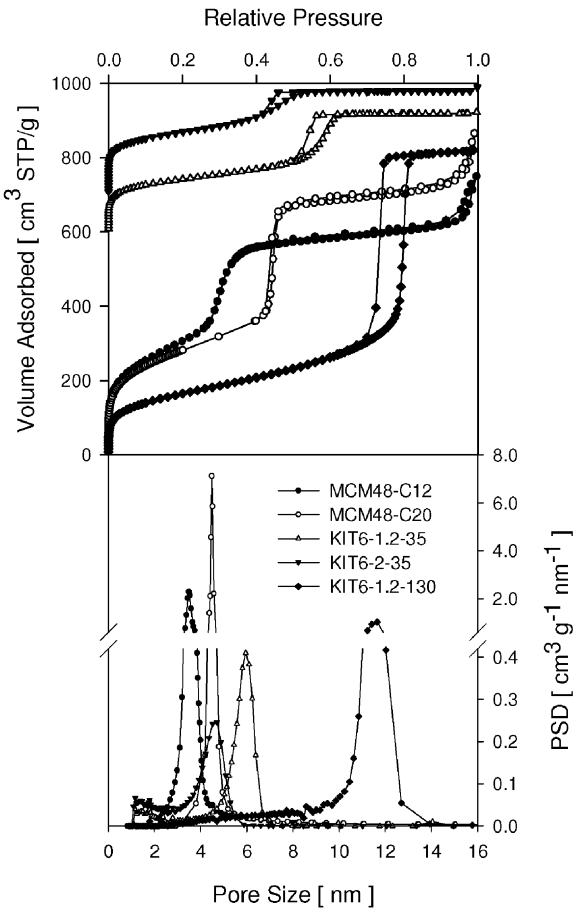

Fig. 1 Nitrogen adsorption isotherms at −196 °C and the corresponding PSDs for ordered mesoporous silica templates used for the synthesis of carbons; the isotherm curves for KIT6-1.2-35 and KIT6-2-35 were offset vertically by 600 and 700 cm^3 STP g^{-1}, respectively.

volume of pores per unit mass of carbon) in relation to that for the carbon templated by silica without textural porosity.[44]

Both KIT6-1.2-35 and KIT6-1.2-130 silicas, synthesized using the same conditions except for the hydrothermal treatment temperature, featured considerably different properties (the synthesis and properties of the KIT-6 silica were reported elsewhere).[33] An increase in the temperature of hydrothermal treatment from 35 to 130 °C caused a substantial enlargement of the size of primary mesopores, from 6.0 to 11.7 nm, followed by ~2.5-fold increase in the pore volume. Both silicas are good quality samples with no textural pores, although the pore size regularity of KIT6-1.2-130 was noticeably better than that of KIT6-1.2-35. In comparison to KIT6-1.2-35, the synthesis of KIT6-2-35 was done at higher TEOS/P123 molar ratio but at the same hydrothermal treatment temperature, and resulted in a smaller pore width and lower uniformity of pores.

Among OMSs studied, KIT6-1.2-130, which was subjected to a high temperature of hydrothermal treatment, possessed full connectivity in the form of interconnecting complementary pores between the interwoven enantiomeric systems of primary channels (mesopores). This feature was reported and confirmed elsewhere[32] by using carbon replication technique; also, it can be inferred from the shape of PSD for this silica having a long tail spreading out from ~2 nm up to the main peak representing primary mesopores (Fig. 1), which indicates a very broad distribution of the complementary pores. It will be shown later that among the silicas studied only this sample can generate a pure $Ia\bar{3}d$ symmetry of the carbon inverse replica. The KIT6-2-35 silica, obtained for a higher ratio of TEOS/P123 in relation to that used for the synthesis of KIT6-1.2-35, had smaller primary mesopores (4.7 nm) and smaller or completely closed interconnecting pores than those present in KIT6-1.2-35. The latter can be evidenced by the properties of carbon inverse replicas of KIT6-1.2-35 and KIT6-2-35, whose structures underwent, respectively, a partial and full symmetry transitions that are characteristic for the CMK-1 carbon.[36] Because the carbon replica of KIT6-2-35 has a relatively large amount of micropores (size < 2 nm) and smaller mesopores, it is more difficult to claim the presence of interconnecting pores in the corresponding silica template solely on the basis of adsorption isotherms.

Adsorption and structural properties of carbons

Table 2, Fig. 2 and 3 show the X-ray diffraction patterns, nitrogen adsorption isotherms and the corresponding pore size distributions as well as adsorption and structural parameters for all carbons studied. As mentioned in the section referring to the silica templates, only carbons (processed at low carbonization temperature) obtained by the use of the KIT-6 sample that was hydrothermally treated at 130 °C retained fully the ordered structure of the template. The CMK8-AN and CMK8-MP OMCs (Fig. 2), synthesized at 900 °C from acenaphthene and mesophase pitch as carbon precursors, exhibited small mesopores (~4.4 nm), which indicates no shift in between separate systems of carbon channels. Also, the small angle XRD pattern, containing (211), (220), (321) peaks, fulfils the $Ia\bar{3}d$ symmetry, which provides solid evidence of the faithful replication of this KIT-6 sample. The example of CMK1-LP-FA carbon synthesized from furfuryl alcohol at 900 °C shows that its structure underwent the aforementioned partial transformation after silica removal. One can infer about this transformation from the XRD pattern, which contains the (211) peak positioned at ~1.2° characteristic for cubic $Ia\bar{3}d$ symmetry and an additional main peak at ~0.7° characteristic for the tetragonal $I4_1/a$ structure. The nitrogen adsorption isotherm for this carbon revealed two capillary condensation–evaporation steps related to two meso pore groups of different sizes, which is reflected by bimodal shape of PSD showing two main peaks located at ~7 and ~10 nm. These data suggest that some complementary pores in the KIT6-1.2-35 template are too small, which makes them insufficient to form strong carbon bridges that are able to sustain the whole structure of the carbon replica. A similar result was also obtained for the CMK1-LP-SU and CMK1-LP-MP samples templated by the same OMS, KIT6-1.2-35, although in this case PSDs do not reveal two well-separated peaks but rather one peak (for large mesopores formed after the structure displacement) with a visible shoulder on its left side. Such shape of PSD is probably a consequence of the difference in the displacement of two interwoven enantiomeric

Table 2 The total pore volume (V_{tot}), BET specific surface area (S_{BET}), external surface area (S_{ext}) and pore size (w_{KJS}) for the carbons studied

Sample	Silica template	V_{tot}/cm^3 g^{-1}	S_{BET}/m^2 g^{-1}	S_{ext}/m^2 g^{-1}	w_{KJS}/nm
OMC that completely lost mesopores and structure (Fig. 2)					
CMK1-C12-FA-900	MCM48-C12	0.93	1130	100	3.65
CMK1-C12-FA-1200		0.75	1250	10	2.71
CMK1-C12-FA-1600		0.78	1250	30	2.51
CMK1-C12-FA-2000		0.60	780	40	2.50
CMK1-C12-FA-2400		0.13	20	—	—
CMK1-C20-FA-900	MCM48-C20	0.91	1050	140	3.22
CMK1-C20-FA-1200		0.89	1060	80	3.36
CMK1-C20-FA-1600		0.86	1070	80	3.30
CMK1-C20-FA-2000		0.66	850	40	2.51
CMK1-C20-FA-2400		0.26	100	40	~3.0
CMK8-AN-900	KIT6-1.2-130	0.44	340	60	4.49
CMK8-AN-1200		0.48	350	60	4.66
CMK8-AN-1600		0.46	360	60	4.48
CMK8-AN-2000		0.24	210	40	3.75
CMK8-AN-2400		0.07	280	—	—
CMK8-MP-900	KIT6-1.2-130	0.34	330	20	4.32
CMK8-MP-1200		0.30	280	10	4.17
CMK8-MP-1600		0.29	320	10	4.03
CMK8-MP-2000		0.14	170	10	3.75
CMK8-MP-2400		0.017	15	—	—
OMC that retained residual mesopores and/or structure (Fig. 3)					
CMK1-LP-SU-900	KIT6-1.2-35	0.89	430	20	12.05
CMK1-LP-SU-1200		0.80	400	20	11.88
CMK1-LP-SU-1600		0.78	360	<10	11.37
CMK1-LP-SU-2000		0.64	290	<10	10.89
CMK1-LP-SU-2400		0.28	120	<10	6.63
CMK1-LP-FA-900	KIT6-1.2-35	1.75	970	20	6.97, 10.03
CMK1-LP-FA-1200		1.67	670	10	6.84, 10.42
CMK1-LP-FA-1600		1.53	870	10	7.04, 10.32
CMK1-LP-FA-2000		1.31	710	20	9.71
CMK1-LP-FA-2400		0.48	360	10	6.69
CMK1-LP*-FA-900	KIT6-2-35	1.49	850	30	10.66
CMK1-LP*-FA-1200		1.34	800	40	9.59
CMK1-LP*-FA-1600		1.26	730	20	10.23
CMK1-LP*-FA-2000		1.05	620	20	9.10
CMK1-LP*-FA-2400		0.52	330	10	6.64
CMK1-LP-MP-900	KIT6-1.2-35	0.44	290	30	8.36
CMK1-LP-MP-1200		0.44	330	40	8.14
CMK1-LP-MP-1600		0.39	290	30	8.16
CMK1-LP-MP-2000		0.32	290	20	4.25, 6.62
CMK1-LP-MP-2400		0.15	120	20	5.76

3D pore structures, which can be due to the use of other carbon precursors than furfuryl alcohol. Particularly, mesophase pitch is a good example showing that its large polyaromatic molecules could penetrate the relatively narrow interconnecting pores in the KIT6-1.2-35 silica to a smaller extent than the molecules of furfuryl alcohol. In comparison to CMK1-LP-FA (900 °C), the CMK1-LP*-FA (900 °C) sample templated by using the KIT6-2-35 silica with higher TEOS/P123 ratio, exhibited a largest displacement of the aforementioned interwoven pore networks, which manifested itself in a unimodal distribution having a peak with a large value of pore width, 10.7 nm and a higher ratio of the XRD intensities of main peaks positioned at ~0.73° and ~1.25°, respectively.

A characteristic feature of almost all the carbons fabricated at 900 °C is a very good ordering of their porous structures inherited from the highly ordered silica templates used. This remarkable ordering of carbons is manifested by a well-defined shape of uniform mesopores having practically no defects in the form of large irregular textural pores created during replication process. Such quality of the carbon replicas can be obtained *via* careful synthesis, which includes a proper adjustment of the amount of carbon precursor to the pore volume of the silica template. An evidence of this careful replication is not only an occurrence of steep capillary condensation and evaporation steps on the nitrogen adsorption isotherms indicating high uniformity of mesopores but also the plateau-like shape of the isotherms that follows this step up to the saturation pressure. If the latter part of the adsorption isotherms for the carbon replica and the corresponding silica template is similar, this is a good indication that the morphology of silica template is retained during the replication process. The aforementioned shape of the adsorption isotherms at the relative pressures greater than ~0.9 is observed for all the carbons studied except that prepared from acenaphthene. A likely reason of this exception lies in the extreme experimental conditions of conversion of acenaphthene into mesophase pitch, which resulted in the exposure of the sample to high vapor pressure of acenaphthene during the conversion process

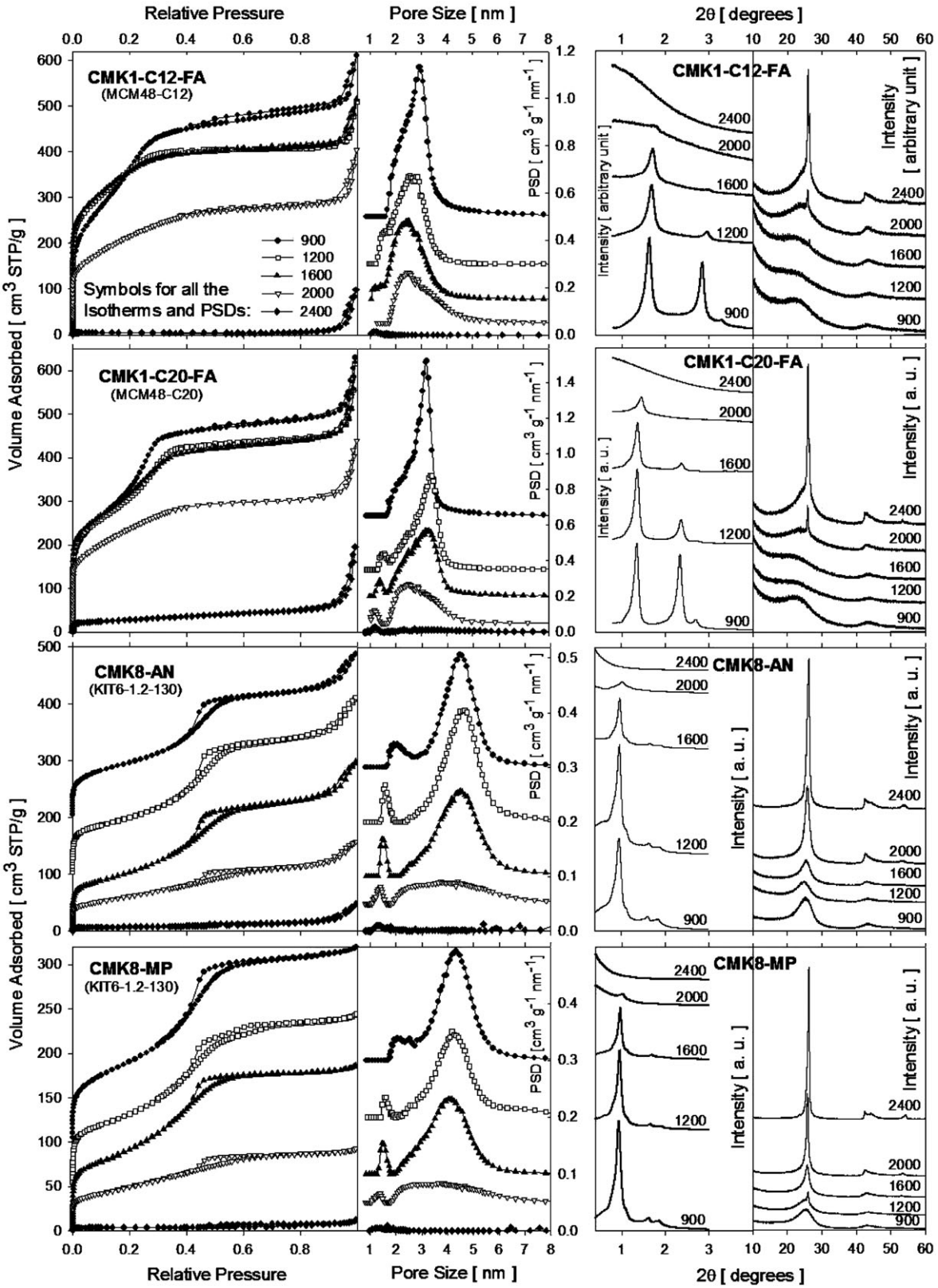

Fig. 2 Nitrogen adsorption, the corresponding pore size distributions (PSDs) and the XRD patterns at small and wide 2θ angles for the series of CMK1-C12-FA, CMK1-C20-FA, CMK8-AN, CMK8-MP carbons thermally treated at 900, 1200, 1600, 2000, 2400 °C. The plots corresponding to the same series of carbons are shown in rows. The columns show, starting from the left side, nitrogen adsorption isotherms at −196 °C, PSD curves, small angle and wide angle XRD patterns. The isotherms for the carbons CMK8-AN-900, CMK8-AN-1200, CMK8-MP-900, and CMK8-MP-1200 were offset vertically by 200, 100, 100 and 50 $cm^3\ g^{-1}$.

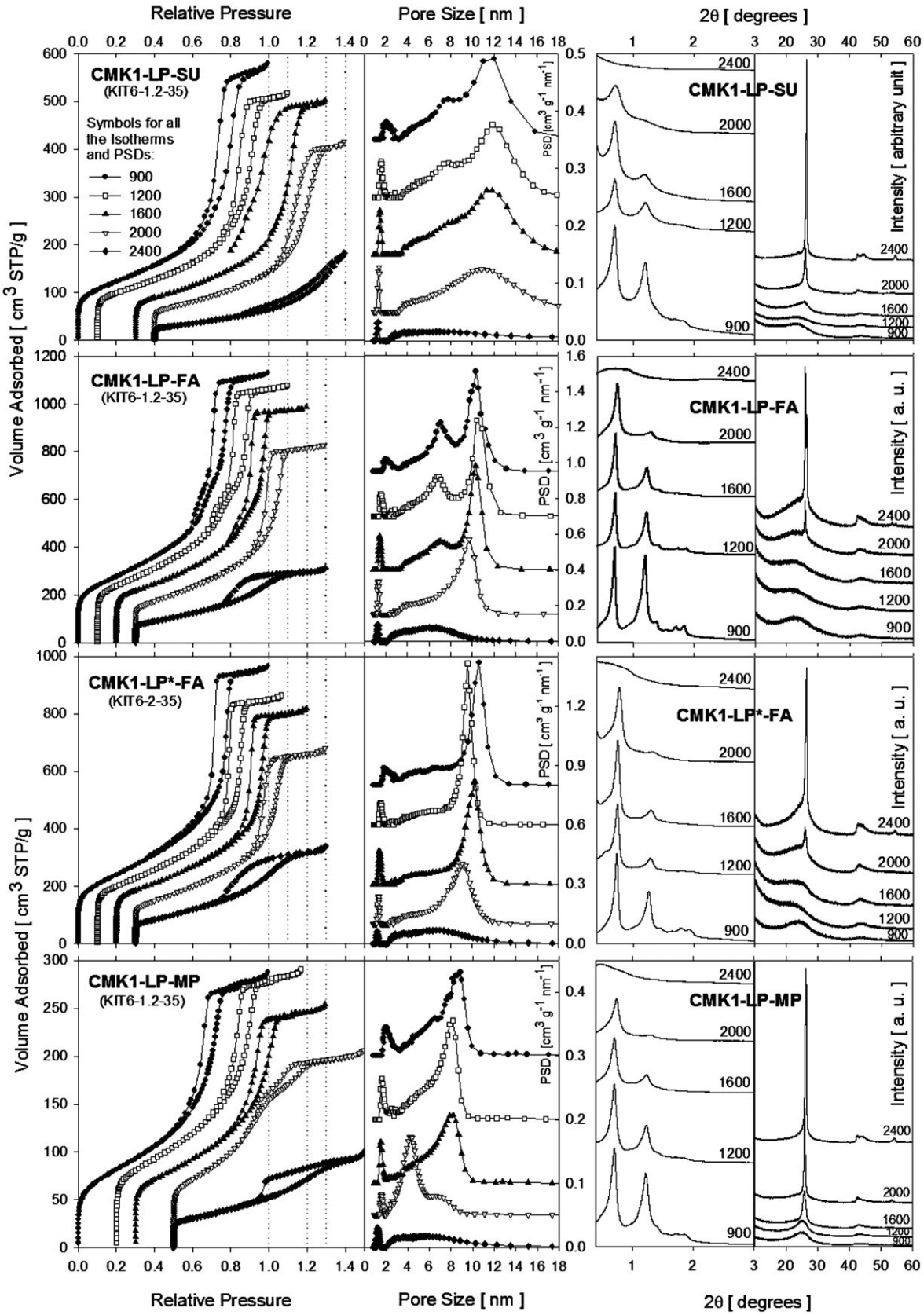

Fig. 3 Nitrogen adsorption, the corresponding pore size distributions (PSDs) and the XRD patterns at small and wide 2θ angles for the series of CMK1-LP-SU, CMK1-LP-FA, CMK1-LP*-FA, CMK1-LP-MP carbons thermally treated at 900, 1200, 1600, 2000, 2400 °C. The plots corresponding to the same series of carbons are shown in rows. The columns show, starting from the left side, nitrogen adsorption isotherms at −196 °C, PSD curves, small angle and wide angle XRD patterns. Several isotherm curves were offset horizontally; the offset values are clearly visible in the figure.

performed in an autoclave at 750 °C. Organic vapors under this condition seemed to cause carbon deposition at the external surface of the template particles.

Fig. 3 contains a set of nitrogen adsorption isotherms, the corresponding PSD curves and XRD patterns for the carbons templated by using KIT6-1.2-35 and KIT6-2-35 OMSs that feature a similar structure. In principle, these carbons were fabricated from two types of carbon precursors: the first type precursors (sucrose and furfuryl alcohol) contain a relatively high percentage of non-carbon elements and the second type precursors (mesophase pitch) have a high percentage of elemental carbon. An essential difference in the adsorption properties of these OMCs (carbonized at 900 °C) is the total pore volume, which was considerably lower for the carbons synthesized from mesophase pitch. Such noticeably low total pore volume has its origin in the nature of this high-coke-yield carbon precursor that generates only a small amount of micropores during carbonization.[12,20] This property could also be found in the case of the other samples, CMK8-AN and CMK8-MP (Fig. 2), exhibiting relatively low total pore and micropore volumes; note that acenaphthene is another example of a high-coke-yield carbon precursor. The influence of carbon precursor on the adsorption properties of resultant carbons has been discussed elsewhere.[13]

Particularly interesting are the results for the carbons subjected to various temperatures of the thermal treatment. The nitrogen adsorption isotherms, PSDs and XRD patterns for all the types of the OMCs studied are shown in Fig. 2 and 3. As can be seen from these figures, there is a substantial drop in the total pore volumes for the carbons subjected to the high temperature thermal treatment in comparison to the corresponding volumes for the carbons treated at 900 °C. An increase in the temperature of thermal treatment from 900 °C to 2400 °C resulted in a gradual decrease in this quantity for most of the carbons studied. An exception was observed for the CMK1-C12-FA and CMK8-AN samples, for which the pore volume increased initially by 4–9% with increasing temperature of the thermal treatment, respectively, from 1200 to 1600 °C and from 900 to 1200 °C (see Table 2).

A significant shrinkage observed for the OMCs studied was caused most likely by three major factors. Namely, thermal treatment caused an essential elimination of micropores from amorphous carbon and contraction of its framework. The other reason is transformation from amorphous carbon to graphite above ~2000 °C, which is associated with carbon densification. However, the most important factor is related to molecular restructuring that took place during graphitization process. Formation of graphene domains in the samples led probably to a fracture of carbon walls that resulted in a loss of porosity after structure disintegration. The fact of structure collapse and the loss of ordering in all graphitized carbons can be evidenced by the aforementioned large decrease in the total pore volume, disappearance or marked broadening of the PSD peaks representing primary mesopores as well as the deterioration of the XRD patterns in the range of small angles.

A controlled temperature treatment allowed us to track the adsorption and structural changes occurring during the heating process. As can be seen from nitrogen adsorption isotherms, a gradual increase in the thermal treatment temperature caused a gradual diminution of the capillary condensation step. This change in the capillary condensation step is reflected by gradual reduction of the PSD peak with increasing temperature but without considerable broadening of its base (broadening would indicate enlargement of some mesopores). This is a sign that the carbons studied underwent a gradually increasing shrinking with increasing treatment temperature, which in turn caused a deterioration of mesopores uniformity. It is noteworthy that the average mesopore size did not change much upon heating the carbon samples up to 2000 °C (except for the CMK1-LP-MP and CMK-8 OMCs, whose properties will be discussed further). A consequence of the aforementioned shrinking was the loss of the nanostructure ordering, particularly well visible on the small angle XRD patterns. These patterns for the CMK-1-type of OMCs reveal a gradual deterioration or disappearance of the reflections with increasing temperature of thermal treatment. The (321) peak centered between 1.5 and 2.0° for the CMK1-LP carbons, and at ~2.7° and ~3.2° for the CMK1-C20 and CMK1-C12 samples, respectively, disappeared after the temperature increase from 900 to 1200 °C. The CMK1-LP-FA-1200 sample that retained the (321) reflection appeared to be more stable and constituted an exception among CMK-1 OMCs. More importantly, the second main peak corresponding to a (211) reflection, in relation to the first one formed after symmetry transition and corresponding to $I4_1/a$ structure, is clearly weakened with increasing temperature and in some cases, such as for CMK1-LP-SU and the carbon replicas of MCM-48, underwent a complete extinction. The series of CMK-8 OMCs exhibited an especially superior thermal stability up to 1600 °C that manifested itself by the preservation of three main XRD peaks, (211), (220) and (321), as well as by the presence of a well-developed PSD peak for the samples treated up to 1600 °C. However, after the treatment at 2000 °C, these carbons drastically lost their porosity along with high degree of ordering. The reason of such a behavior is described further.

In general, a relatively high thermal stability up to 2000 °C is observed for the CMK-1 type of carbons that underwent a symmetry transition (except the CMK1-C12-FA-2000 sample). These carbons exhibited prominent adsorption and structural parameters even after thermal treatment at 2000 °C, featuring high pore volume (0.32–1.31 $cm^3\ g^{-1}$), specific surface area (290–850 $m^2\ g^{-1}$) and, what is equally important, the well-preserved ordered mesostructure, as judged by XRD patterns (see Fig. 2).

Among the MCM-48-templated carbons treated at 2000 °C, CMK1-C20-FA and less thermally stable CMK1-C12-FA had pore volumes of 0.66 and 0.60 $cm^3\ g^{-1}$ as well as high surface areas of 850 and 780 $m^2\ g^{-1}$, respectively. For these samples the average size of mesopores decreased to about 70 and 80% of the initial value, respectively, achieving 2.5 nm. The small angle XRD patterns indicate some deterioration of mesostructural ordering that was especially significant in the case of CMK1-C12-FA-2000, for which only one very small peak positioned at ~1.75° is visible.

Further interesting results are shown in Fig. 3 for the CMK1-LP-SU, CMK1-LP-FA and CMK1-LP*-FA carbons. The large pore volumes for the latter two samples treated at

900 °C, 1.75 and 1.49 $cm^3\ g^{-1}$, respectively, decreased only by about 25–20% after treatment at 2000 °C, which is an indication of relatively small shrinkage. Also their surface areas remained considerably high, whereas the mesopore size changed slightly by only 3 and 15%, respectively. In the case of CMK1-LP-FA-2000, one can notice disappearance of one PSD peak for smaller (~7 nm) mesopores from bimodal PSD obtained for the CMK1-LP-FA-900 carbon. The reason for that lies in the structure of CMK1-LP-FA-900 which features a partial symmetry transition only. Because of the carbon wall displacement causing the aforementioned symmetry transition, a part of its pores underwent enlargement, while the other part, visible on the PSD curve in the form of a peak located at ~7 nm, remained intact reflecting the faithful inverse structure of the silica template. Under the influence of high temperature of 2000 °C, very thin bridges interconnecting the primary carbon walls fractured, which could extend the aforementioned symmetry transition to the entire volume of the sample. This process could be intensified by the obvious volume contraction. An additional evidence for adsorption analysis of the CMK1-LP-FA-2000 and CMK1-LP*-FA-2000 samples is provided by the XRD patterns, which feature one pronounced sharp peak located at ~0.75° and the other low intensity peak at ~1.3° that point out the preservation of mesostructural ordering. The XRD data together with nitrogen adsorption isotherms indicate a good quality of these OMC samples treated at high temperature of 2000 °C.

The thermal behavior of the CMK-8 carbons (Fig. 2) clearly differs from that for CMK-1 (except CMK1-C12-FA-2000). This difference is related to the structure of the former samples being the faithful inverse replica of the KIT-6 silica template. The PSD peaks for these carbons treated at 2000 °C were noticeably broader compared to those for the CMK-1-type structures. Likely, the reason for that behavior is analogous to the situation observed in the case of the CMK1-LP-FA-2000 sample. Namely, the high temperature of thermal treatment probably led to a fracture of certain parts of interconnecting carbon bridges in the CMK-8 carbons, which caused the structure disintegration and in consequence the loss of porosity. The small angle XRD patterns for these samples showed only one very weak peak at ~1.0°, which confirmed a drastically poorer nanostructural ordering. This finding along with adsorption data allows us to infer that the CMK-8 carbons underwent a considerate structural deterioration. Additionally, disintegration of the carbon bridges caused only a partial displacement of carbon nanowalls in CMK-8, which manifested itself in basically unchanged base width of much smaller PSD peak. This, in turn, indicates the retention of the pore size and a decrease in total pore volume. The results obtained for the CMK-8-type of OMCs, which are structurally similar to CMK1-LP-FA, seem to be consistent and allow us to conclude that both porous structures experienced similar changes upon the heat treatment at 2000 °C.

One of the most relevant results was acquired for the carbons subjected to the highest applied temperature, 2400 °C, allowing an appreciable degree of graphitization to be achieved. Analysis of data shown in Fig. 2 indicates that the MCM-48-templated CMK-1 carbons and the CMK-8 carbons possessed comparable adsorption and structural properties. Namely, all these samples underwent a virtually complete disintegration upon graphitization. The small angle XRD patterns for these samples are featureless indicating a complete loss of the nanostructural ordering. In the case of the CMK-8 carbons, adsorption analysis revealed almost complete loss of porosity, which is confirmed by a complete disappearance of the PSD peak related to mesopores that were present in the carbons heated at 2000 °C. Likewise, CMK1-C12-FA and CMK1-C20-FA had no such PSD. Their residual porosity (pore volume of 0.13 and 0.26 $cm^3\ g^{-1}$, respectively) was obtained because of the carbon structure collapse and consisted of large-size irregular mesoporous defects.

Wide angle XRD patterns (in the range of 10°–60°) provided additional valuable information about the crystalline structure of the carbon pore walls formed during graphitization. The XRD patterns shown in Fig. 2 for the samples graphitized at 2400 °C feature well-defined intense peaks at ~26°, ~43° and ~54° that correspond, respectively, to (002), (100)/(101) (superposition of two XRD reflections), and (004) reflections characteristic for the graphite. From XRD data for the carbons synthesized from furfuryl alcohol, one can infer that a certain amount of graphitic domains in the framework was formed at 2000 °C. Two clear (002) and (100)/(101) peaks are present on the XRD patterns for these samples. In the case of CMK1-C20-FA heated at 1600 °C, a very weak but sharp (002) peak was observed, which suggests that graphitization process occurred to a small extent at such relatively low temperature. In comparison to the furfuryl alcohol-based graphitized carbons, those synthesized from polyaromatic acenaphthene and mesophase pitch exhibited decidedly better crystalline properties. The XRD patterns with three (002), (100)/(101), and (004) peaks are already observed for the carbon samples heated at 2000 °C, whereas a temperature as low as 1200 °C turned out to be sufficient to produce the small fraction of graphitic domains in the mesophase pitch-based carbons as revealed by a low-intensity sharp (002) peak. The CMK-8 samples, for which intense XRD peaks with a very narrow-base are observed, show that the carbons synthesized from polyaromatic compounds feature long-range graphite-like ordering after graphitization at 2400 °C.

All carbon samples heated at 2000 and 2400 °C have a sharp (002) peak. For the pitch-based carbons this peak is already quite sharp for the samples heated at 1600 °C, indicating high susceptibility of MP and AN carbon precursors towards graphitization. Table 3 provides the values of the interlayer spacing d_{002} for the aforementioned carbon samples, *i.e.*, those for which the (002) peak is sharp. Also, for those carbon samples we evaluated the stacking height of graphitic domains using the Scherrer equation: $L_c = k\,\lambda/(B\cos\theta)$, where λ is the wavelength of the X-rays, B is the peak width (full width at half height in radians), θ is the angle at which a given reflection is observed, and k is a constant.[45] Following Knox *et al.*[19] $k = 0.84$ was used for evaluation of the stacking height of the graphitic domains from the width of the (002) reflection.

As can be seen from Table 3 the interlayer spacing values are about 0.34 nm, which is similar to that of 0.335 nm in natural graphite. However, the values of the stacking height of graphitic domains seem to be too large in relation to the pore wall thickness, especially for the FA and SU-based carbons.

Table 3 The structural parameters of graphitic domains evaluated on the basis of the (002) peak for all carbons samples heated at 2000 and 2400 °C and the AN- and MP-based carbon samples heated at 1600 °C

Carbon sample	Interlayer spacing d_{002}/nm	Stacking height L_c/nm
CMK1-C12-FA-2000	0.343	22
CMK1-C12-FA-2400	0.343	22
CMK1-C20-FA-2000	0.344	25
CMK1-C20-FA-2400	0.343	25
CMK8-AN-1600	0.346	2.8
CMK8-AN-2000	0.345	5.9
CMK8-AN-2400	0.340	9.5
CMK8-MP-1600	0.345	5.6
CMK8-MP-2000	0.344	11
CMK8-MP-2400	0.339	14
CMK1-LP-SU-2000	0.344	13
CMK1-LP-SU-2400	0.337	23
CMK1-LP-FA-2000	0.344	27
CMK1-LP-FA-2400	0.344	26
CMK1-LP*-FA-2000	0.343	9.5
CMK1-LP*-FA-2400	0.339	15
CMK1-LP-MP-1600	0.343	6.8
CMK1-LP-MP-2000	0.343	18
CMK1-LP-MP-2400	0.339	20

These relatively large graphitic domains can be formed due to a partial or complete collapse of the porous carbon structure during graphitization (a complete collapse occurred for the carbons graphitized at 2400 °C shown in Fig. 2), structure displacement resulting in the thicker pore walls, and/or preferential orientation of graphene sheets. When the broad component of the (002) peak was used for the estimation of the stacking height,[24] much smaller values of $L_c = \sim 1.0$–1.8 nm were obtained.

The degree of graphitization can also be monitored by means of low pressure nitrogen adsorption at −196 °C. Adsorption of nitrogen molecules on the highly graphitized carbons proceeds through layer-by-layer formation that is commensurate to the surface structure. An S-shape of the low pressure adsorption isotherm presented in semi-logarithmic scale on highly graphitized carbons indicates their high surface homogeneity. The examples of low pressure adsorption graphs that demonstrate this phenomenon are shown in Fig. ESI-1†, which contains the surface coverage curves (surface coverage was obtained by dividing the amount of adsorbed nitrogen by the BET monolayer capacity) for selected carbon samples. These curves for the CMK1-C20-FA and CMK8-AN carbons graphitized at 2400 °C feature S-shape behavior typical for nitrogen adsorption on the graphitic surface located at a relative pressure in the range of 10^{-4}–10^{-3} reflecting the monolayer formation. As can be seen this S-shape behavior is particularly distinct for the samples obtained at the highest carbonization temperature, indicating their high surface homogeneity, and consequently high degree graphitization.[46]

A separate group of graphitized carbons, for which nitrogen adsorption isotherms, PSD curves and XRD patterns are shown in Fig. 3, appears to have different properties than the carbons listed in Fig. 2. The most distinctive feature of the former is their considerably higher total pore volume and specific surface area. They include the CMK1-LP-SU, CMK1-LP-FA and CMK1-LP*-FA samples synthesized from non-aromatic carbon precursors, which after graphitization at 2400 °C exhibited the pore volume of 0.28 $cm^3\ g^{-1}$, 0.48 $cm^3\ g^{-1}$ and 0.52 $cm^3\ g^{-1}$, respectively (see Table 2). These values for furfuryl alcohol-based carbons were approximately twice as large as the pore volumes of the MCM-48-templated carbon, CMK1-C20-FA-2400. The specific surface areas for the aforementioned carbons were particularly large and equal to 120, 360 and 330 $m^2\ g^{-1}$, respectively. In the case of the CMK1-LP-MP-2400 carbon synthesized from mesophase pitch, these quantities were equally large (0.15 $cm^3\ g^{-1}$ and 120 $m^2\ g^{-1}$) as for a high-coke-yield carbon precursor. In contrast to the group of graphitized carbons collected in Fig. 2, nitrogen adsorption isotherms for furfuryl alcohol- and mesophase pitch-based carbons (Fig. 3) possess capillary condensation steps followed by plateau-like isotherm shape. Their PSDs feature a small broad peak in the range of mesopores from ~2 nm to ~10–12 nm. In general, adsorption data show that these carbons graphitized at 2400 °C preserved around 30% of the pore volume observed for the same samples carbonized at 900 °C and still contained a residual fraction of regular mesopores. Also, small angle XRD data acquired for this group of carbons are of somewhat better quality. Excluding the CMK1-LP-SU-2400 sample shown in Fig. 3, the XRD patterns feature a broad peak for the CMK1-LP-FA and CMK1-LP-FA* graphitized carbons, or a distinct shoulder, below 1°. This study shows that the graphitization at 2400 °C led to a serious deterioration of structural properties of the carbons studied manifesting itself in the disappearance of intense XRD peaks at small angles but still some residual nanostructure ordering was retained as evidenced by nitrogen adsorption analysis. The wide angle XRD patterns shown in Fig. 3 reveal the highest degree of graphitization in this group of samples for CMK1-LP-SU-2400 that did not have any nanostructural ordering or uniform mesopores. Its diffraction pattern features (up to 60°) an intense (002) peak with a very small width at the base, two separated (001) and (101) peaks at ~42.5° and ~44°, respectively, and (004) reflection. This sample exhibited some partial ordering starting from temperature of 2000 °C. The XRD patterns for all the other carbons heated at 2400 °C feature three (002), (001)/(101), (004) peaks and at least two peaks are present for carbons heated at 2000 °C. As mentioned in the case of CMK8-MP-2000, also the CMK1-LP-MP-2000 carbon obtained from polyaromatic mesophase pitch at 2000 °C exhibited similar crystalline properties having three characteristic reflections. Shown in Fig. 4 TEM images for the CMK1-LP-MP-900 and −2000 carbons indicate that the graphitization at 2000 °C preserves structural ordering and improves crystallinity of the pore walls. To support the above conclusions about graphitization of the CMK1-LP*-FA and CMK1-LP-MP carbons the low pressure nitrogen adsorption isotherms are shown in Fig. ESI-1†, indicating a distinct S-shape for the samples heated at 2400 °C. As can be seen in this figure for a series of furfuryl alcohol-based CMK1-LP*-FA carbons, the low pressure isotherms for the samples heated at 2000 and 2400 °C feature an approximate curvature, which indicates that these two samples had similar surface properties.

An additional confirmation of high degree graphitization of the carbons heated at 2000 and 2400 °C is provided by

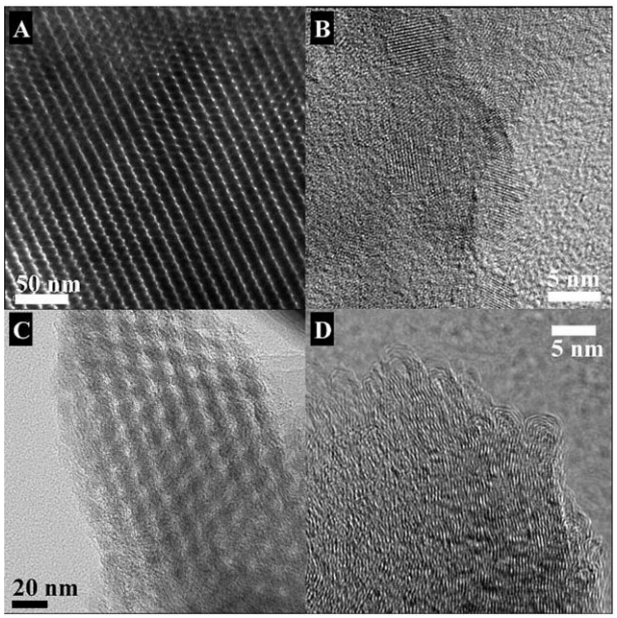

Fig. 4 TEM images for CMK1-LP-MP carbonized at 900 °C (panels A and B) and graphitized at 2000 °C (panels C and D).

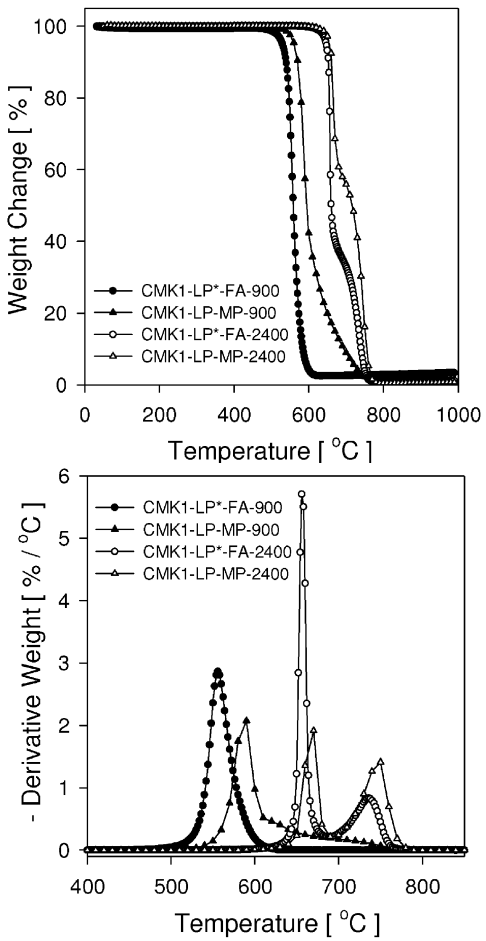

Fig. 5 Comparison of the TG (top) and DTG (bottom) profiles recorded in flowing air for the CMK1-LP*-FA and CMK1-LP-MP carbons prepared at 900 and 2400 °C.

thermogravimetric analysis of these samples in air. Fig. 5, ESI-2 and ESI-3† show the weight change (TG) and differential (DTG) profiles for the CMK1-LP*-FA and CMK1-LP-MP samples prepared at 900, 2000 and 2400 °C. In contrast to a single-step TG profile (single DTG peak) for the samples carbonized at 900 °C, the TG profiles for the carbons graphitized at 2000 and 2400 °C show a two-step oxidation (bimodal DTG curve) as reported elsewhere.[7] The TG weight loss at lower temperature reflects the oxidation of amorphous carbon, whereas the step at higher temperature is related to the oxidation of graphitic domains.[7] As can be seen from Fig. 5, ESI-2 and ESI-3† showing the TG and DTG profiles for the FA- and MP-based carbons, the oxidation steps shift towards higher temperatures with increasing temperature of graphitization. Also, the height of the second step increases with increasing temperature of graphitization, reflecting an increase in the crystallinity of carbon matrix. For instance, the TG profiles for the CMK1-LP*-FA and CMK1-LP-MP carbons graphitized at 2000 °C give the weight loss values of 17% and 33%, respectively, whereas, those at 2400 °C give, respectively much higher values, 35% and 49%. These data show that the carbons prepared from mesophase pitch exhibit higher degree of crystallinity in comparison to those obtained from furfuryl alcohol.

Finally, shown in Fig. ESI-4† are the Raman spectra for the CMK1-LP*-FA and CMK1-LP-MP carbons prepared at 900, 2000 and 2400 °C. As expected these spectra exhibit two D (1350 cm^{-1}) and G ($\sim$1580 cm^{-1}) bands related to the disordered and graphitic domains.[47] The integrated intensity ratio for the D and G bands, I_D/I_G, decreases with increasing graphitization temperature, indicating an enlargement of graphitic domains; however, for the samples studied the TG analysis seems to be more informative than the Raman spectra.

Conclusions

In summary, the data shown in Fig. 2 and 3 for all the series of the thermally treated carbons indicate that the degree of graphitization depends insignificantly on the type of carbon precursor at temperature 2400 °C or higher; the effect of carbon precursor becomes more and more pronounced at decreasing temperature of the thermal treatment. The porous and structural properties of the graphitized carbons were strongly affected by the heat treatment at 2400 °C. Generally, this high temperature treatment resulted in the development of crystalline carbon framework but, on the other hand, it led to a significant shrinkage, partial or complete disappearance of uniform mesopores and, in consequence, to a significant deterioration of the nanostructural ordering or its complete loss. It was found that the thermal stability of the carbons, besides the carbon sources, depends in the largest measure on the structural properties inherited from the silica templates. One group of the carbons studied (Fig. 2) lost both the nanostructural ordering and porosity, while the other group retained at least one of these properties in a residual form (Fig. 3). The first group (Fig. 2) includes the MCM-48-templated carbons (CMK1-C12-FA, CMK1-C20-FA) that underwent a symmetry transition after template removal and

the CMK8-AN and CMK8-MP carbons templated by using a large pore KIT-6 silica; the latter were a faithful inverse replica of the KIT-6 template used.

The second group (Fig. 3) includes more thermally stable carbons, templated by a relatively small pore KIT-6 silica that underwent complete (CMK1-LP-SU, CMK1-LP*-FA, CMK1-LP-MP) and partial (CMK1-LP-FA) symmetry transitions after template removal. The aforementioned symmetry transition occurred due to the lack of bridges (as in the case of CMK1-C12-FA and CMK1-C20-FA) or sufficiently strong bridges interconnecting the walls of the primary mesopores, which was the direct consequence of the structural properties of the MCM-48 and small pore KIT-6 silica templates used. The observed deterioration of adsorption and nanostructural properties of the carbons subjected to heating at 2400 °C was most likely caused by restructuring of amorphous carbon framework of high curvature to graphite. During this process the carbon pore walls alone as well as those with interconnecting bridges fractured resulting in structure disintegration at the nanoscale level. However, in the case of large-pore CMK-1 samples, some portion of the residual mesoporosity still remained even after graphitization at 2400 °C.

Acknowledgements

This work was supported in part by the Korea National Honor Scientist program (R.R.), the Brain Korea 21 project (R.R.) and in part through subcontract (M.J.) under the NIRT DMR-0304508 grant from NSF awarded to the Carnegie Mellon University. The authors acknowledge support from Pohang Light Source for synchrotron radiation XRD measurements and from National Nanofab Center for TEM measurements. The authors also thank Mitsubishi Gas Chemical Co. for the donation of the AR mesophase pitch.

References

1 R. Ryoo, S. H. Joo, M. Kruk and M. Jaroniec, *Adv. Mater.*, 2001, **13**, 677.
2 J. Lee, J. Kim and T. Hyeon, *Adv. Mater.*, 2006, **18**, 2073.
3 A.-H. Lu and F. Schüth, *Adv. Mater.*, 2006, **18**, 1793.
4 B. Lebeau, J. Parmentier, M. Soulard, C. Fowler, R. Zana, C. Vix-Guterl and J. Patarin, *Chimie*, 2005, **8**, 597.
5 B. Sakintuna and Y. Yurum, *Ind. Eng. Chem. Res.*, 2005, **44**, 2893.
6 S. B. Yoon, J. Y. Kim, J.-S. Yu, K. P. Gierszal and M. Jaroniec, *Ind. Eng. Chem. Res.*, 2005, **44**, 4316.
7 A. B. Fuertes and T. A. Centeno, *J. Mater. Chem.*, 2005, **15**, 1079.
8 C.-M. Yang, C. Weidenthaler, B. Spliethoff, M. Mayanna and F. Schüth, *Chem. Mater.*, 2005, **17**, 355.
9 C. H. Kim, D.-K. Lee and T. J. Pinnavaia, *Langmuir*, 2004, **20**, 5157.
10 C. Vix-Guterl, S. Saadallah, L. Vidal, M. Reda, J. Parmentier and J. Patarin, *J. Mater. Chem.*, 2003, **13**, 2535.
11 H. Yang, Y. Yan, Y. Liu, F. Zhang, R. Zhang, Y. Meng, M. Li, S. Xie, B. Tu and D. Zhao, *J. Phys. Chem. B*, 2004, **108**, 17320.
12 Z. Li and M. Jaroniec, *J. Am. Chem. Soc.*, 2001, **123** 9208.
13 K. P. Gierszal, T.-W. Kim, R. Ryoo and M. Jaroniec, *J. Phys. Chem. B*, 2005, **109**, 23263.
14 T.-W. Kim, I.-S. Park and R. Ryoo, *Angew. Chem., Int. Ed.*, 2003, **42**, 4375.
15 H. Darmstadt, C. Roy, S. Kaliaguine, S. H. Joo and R. Ryoo, *Microporous Mesoporous Mater.*, 2003, **60**, 139.
16 Y. Xia and R. Mokaya, *Adv. Mater.*, 2004, **16**, 1553.
17 P. J. F. Harris, *Crit. Rev. Solid State Mater. Sci.*, 2005, **30** 235.
18 O. P. Krivoruchko, N. I. Maksimova, V. I. Zaikovskii and A. N. Salanov, *Carbon*, 2000, **38**, 1075.
19 J. H. Knox, B. Kaur and G. R. Millward, *J. Chromatogr.*, 1986, **352**, 3.
20 Z. Li and M. Jaroniec, *Anal. Chem.*, 2004, **76**, 5479.
21 Z. Li, M. Jaroniec, Y. J. Lee and L. R. Radovic, *Chem. Commun.*, 2002, 1346.
22 A. B. Fuertes and S. Alvarez, *Carbon*, 2004, **42**, 3049.
23 S. B. Yoon, G. S. Chai, S. K. Kang, J.-S. Yu, K. P. Gierszal and M. Jaroniec, *J. Am. Chem. Soc.*, 2005, **127**, 4188.
24 M. Kruk, K. M. Kohlhaas, B. Dufour, E. B. Celer, M. Jaroniec, K. Matyjaszewski, R. S. Ruoff and T. Kowalewski, *Microporous Mesoporous Mater.*, 2007, **102**, 178.
25 A.-H. Lu, W.-C. Li, E.-L. Salabas, B. Spliethoff and F. Schüth, *Chem. Mater.*, 2006, **18**, 2086.
26 C. Liang, S. Dai and G. Guiochon, *Anal. Chem.*, 2003, **75** 4904.
27 S. Han, Y. Yun, K.-W. Park, Y.-E. Sung and T. Hyeon, *Adv. Mater.*, 2003, **15**, 1922.
28 M. Sevilla and A. B. Fuertes, *Carbon*, 2006, **44**, 468.
29 J. N. Wang, L. Zhang, J. J. Niu, F. Yu, Z. M. Sheng, Y. Z. Zhao, H. Chang and C. Pak, *Chem. Mater.*, 2007, **19**, 453.
30 Z. Lei, Y. Xiao, L. Dang, W. You, G. Hu and J. Zhang, *Chem. Mater.*, 2007, **19**, 477.
31 J. S. Beck, J. C. Vartuli, W. J. Roth, M. E. Leonowicz, C. T. Kresge, K. D. Schmitt, C. T.-W. Chu, D. H. Olson, E. W. Sheppard, S. B. McCullen, J. B. Higgins and J. L. Schlenker, *J. Am. Chem. Soc.*, 1992, **114**, 10834.
32 F. Kleitz, S. H. Choi and R. Ryoo, *Chem. Commun.*, 2003, 2136.
33 T.-W. Kim, F. Kleitz, B. Paul and R. Ryoo, *J. Am. Chem. Soc.*, 2005, **127**, 7601.
34 D. Zhao, Q. Huo, J. Feng, B. F. Chmelka and G. D. Stucky, *J. Am. Chem. Soc.*, 1998, **120**, 6024.
35 S. Jun, S. H. Joo, R. Ryoo, M. Kruk, M. Jaroniec, Z. Liu, T. Ohsuna and O. Terasaki, *J. Am. Chem. Soc.*, 2000, **122**, 10712.
36 R. Ryoo, S. H. Joo and S. Jun, *J. Phys. Chem. B*, 1999, **103**, 7743.
37 T. W. Kim and L. A. Solovyov, *J. Mater. Chem.*, 2006, **16**, 1445.
38 R. Ryoo, S. H. Joo and J. M. Kim, *J. Phys. Chem. B*, 1999, **103**, 7435.
39 M. Kruk, M. Jaroniec, R. Ryoo and S. H. Joo, *Chem. Mater.*, 2000, **12**, 1414.
40 R. Ryoo, C. H. Ko and I.-S. Park, *Chem. Commun.*, 1999, 1413.
41 (*a*) R. Ryoo, S. Jun, J. M. Kim and M. J. Kim, *Chem. Commun.*, 1997, 2225; (*b*) S. Jun and R. Ryoo, *J. Catal.*, 2000, **195**, 237.
42 S. H. Joo, S. Jun and R. Ryoo, *Microporous Mesoporous Mater.*, 2001, **44–45**, 153.
43 M. Kruk, M. Jaroniec and A. Sayari, *Langmuir*, 1997, **13**, 6267.
44 K. P. Gierszal and M. Jaroniec, *J. Phys. Chem. C*, 2007, **111**, 9742.
45 P. Scherrer, *Nachr. Ges. Wiss. Gottingen*, 1918, 96.
46 M. Kruk, Z. Li, M. Jaroniec and W. R. Betz, *Langmuir*, 1999, **15**, 1435.
47 M. A. Pimenta, G. Dresselhaus, M. S. Dresselhaus, L. G. Cancado, A. Jorioa and R. Saitoe, *Phys. Chem. Chem. Phys.*, 2007, **9**, 1276.